

Diffusion Coefficients of the 45S and 50S States of the Large Ribosomal Subunit of *E. coli* by Quasielastic Light Scattering*

Charles C. Han

Center for Materials Science, National Bureau of Standards, Washington, DC 20234

I. N. Serdyuk** and Hyuk Yu

Department of Chemistry, University of Wisconsin, Madison, Wisconsin 53706

October 3, 1978

The translational diffusion coefficients of the 45S and 50S states of the large ribosomal subunit of *E. coli* were determined from the spectral distributions of quasielastically scattered light with a 5 mW He-Ne laser as the source. The spectral analysis was performed by directly Fourier transforming the photocurrent and fitting to double-Lorentzian profile via a non-linear regression routine. A small amount (about 1%) of strongly scattering contaminants required the double-Lorentzian profile in order to extract the diffusion coefficients of the principal components. The results are: D_{20}° , w(45S) = $(1.79 \pm 0.12) \times 10^{-7} \text{cm}^2/\text{sec}$, and D_{20}° , w(50S) = $(1.91 \pm 0.06) \times 10^{-7} \text{cm}^2/\text{sec}$, the latter being in accord with those reported in the literature. The transition from the 50S state to the 45S state is not attended by a change in its molecular weight if the partial specific volumes are assumed to be the same.

Key words: Diffusion coefficient; *E. coli* ribosomal subunit; 45S and 50S; quasielastic light scattering.

1. Introduction

The most immediate task in characterizing complex sub-cellular particles such as ribosomes, is to assign molecular weights. This is commonly performed by determining the sedimentation and diffusion coefficients in conjunction with the partial specific volume. With the advent of the laser light scattering technique, [1]¹ the diffusion coefficients of a variety of subcellular particles, viruses, and macromolecules [2] have been determined at a substantial savings in effort and time, though not necessarily with improved precision over conventional techniques. As diffusion coefficients become more readily available, molecular weight assignments will be less time consuming. Interest in the diffusion coefficient also resides in deducing the geometric eccentricity [3] of a uniform density particle by comparing the equivalent Stokes radius to the radius of gyration obtained by the scattering intensity technique with X-ray, slow (or cold) neutron, or visible light. Conversely the component density segregation within a particle can be inferred when the Stokes

radius deduced from the diffusion coefficient is larger than the radius of gyration. Such an inference was drawn by Serdyuk *et al.* [4] with the 50S subunit from the study of small angle X-ray scattering and the diffusion coefficient.

In this paper, we report a study of the diffusion coefficients of the 50S and 45S states of the large ribosomal subunit using quasielastic light scattering (QEL). The purpose is two fold. First, we show that the two states, which differ by 5 Svedberg units, can be distinguished by the diffusion coefficient as obtained by the technique. Second, a method for extracting individual spectral halfwidths, hence diffusion coefficients, from a bimodally distributed scattering system is put forth. The scheme is analogous to the one adopted by Bargeron [5] except that ours is in the frequency domain while his is in the time domain.

In the determination of the translational diffusion coefficient by QEL, a trace amount of contaminants having a larger dimension than that of the principal component poses a major experimental problem. This is simply due to the larger scattering intensity of the impurity component which obscures the scattering contribution of the principal one. This sort of polydispersity effect has been the cause of a good deal of examination in test systems recently [5-8]. It is generally agreed that one indeed measures the z-average quantity [8-10] of the diffusion coefficient when the intraparticle form factor is unity as first shown by Koppel [11].

* Certain commercial materials and equipment are identified in this paper in order to specify adequately the experimental procedure. In no case does such identification imply recommendation or endorsement by the National Bureau of Standards, nor does it imply that the material or equipment identified is necessarily the best available for this purpose.

** Permanent Address: Institute of Protein Research, Academy of Sciences of the U.S.S.R., Poustchino, Moscow Region, U.S.S.R.

¹ Figures in brackets indicate literature references at the end of this paper.

Hence the data analysis of the spectral profile of scattered light from a bimodally distributed system compared to a smoothly distributed system requires some care, particularly when one is interested in a small component that is contaminated by even trace amounts of a large component. Depending on the ratio of linear dimensions of the two, one can easily be misled by the z-average quantity that is predominantly weighted by the larger component [12]. We show here that the spectral analysis has been successfully carried out in determining the diffusion coefficients of the 45S and 50S states of the large ribosomal subunit contaminated by some larger particles, from sources as yet undetermined. The contaminant components appeared to be 6 to 7 times greater in diffusion coefficients than the principal ones, but present in no more than a few parts per hundred by weight.

2. Experimental

2.1 Sample preparation

The ribosomal subunits were extracted from the MRE-500 strain of *E. coli* in Professor Spirin's laboratory at the Institute of Protein Research, The Academy of Sciences, U.S.S.R. by a modified version of the method reported previously by Gavrilova *et al.* [12] with the use of B-XV zonal rotor of a MSE* superspeed 65 preparative ultracentrifuge. All solutions were prepared immediately before the experiments from the ribosome preparations stored in saturated ammonium sulfate. The 50S ribosomal subunit solution was prepared as follows. The ribosome suspension was centrifuged for 25 minutes at 1.7×10^4 g to pellet. After the supernatant liquid was decanted, the pellet was resuspended in a few ml of the buffer (0.07 M KCl, 0.01 M tris-HCl, 1 mM Mg^{+2} , pH 7.1) and dialyzed for eight hours against the same buffer with threefold exchange. The 45S state of the subunit was prepared from a 50S subunit solution by dialysis against the following buffer: (0.5 M NH_4Cl , 0.01 M tris-HCl, 1 mM Mg^{+2} , pH 7.1).

2.2 Sample Clarification

The subunit solutions at a nominal concentration of $2 \text{ mg} \cdot \text{ml}^{-1}$ were centrifuged on a preparative centrifuge for 1–2 h at 6.7×10^3 g before subjecting them to light scattering. In one case, we further clarified the solution by filtering through $0.1 \mu\text{m}$ Nucleopore* filter without imposing a positive pressure gradient upstream. Although the Schlieren patterns of the solutions before and after the scattering invariably produced a homogeneous single peak, the spectral analysis required the double-Lorentzian scheme (see below).

2.3 Light Scattering

The instrument for this study has been described elsewhere [13]. The laser source of the instrument is a 5 mW He-Ne laser (Spectra-Physics 135)*. The time varying output of a photomultiplier (RCA C7164R)* produced by the homodyne beating of the scattered optical field at the photocathode [14] is converted to voltage, amplified by a wide-band device, band limited to frequencies below the Nyquist limit of one-half the sampling frequency by a filter (Dytronics 722)*, sampled and digitized at an appropriate rate controlled by a real time clock, then directly Fourier transformed, and accumulated on an on-line minicomputer (PDP8/E)*. Over a given bandwidth (2.5 KHz and 10 KHz for this study), the power spectrum is constituted of 256 power coefficients that are averaged over 2000–4000 scans. After correcting for the instrumental profile, the spectrum is then analyzed by fitting it to model profiles via a non-linear regression routine [15].

The scattering angles were incremented by 15° from 45° – 90° and finally by 20° to 110° for both 45S and 50S solutions, and an additional angle at 30° for the latter was examined. Temperature of the scattering cell (10 mm NMR tube) immersed in a refractive index matching liquid (Silicone oil) was not controlled away from the ambient but continually monitored with a calibrated quartz thermometer (Hewlett-Packard 2801A)*. For a given run of scattering, the temperature variation was noted to be within 0.2°C .

2.4 Data Analysis

For a bimodally distributed scattering system, the scattered power spectrum in the frequency domain is given by the following equations, [14] provided (1) the optical field is governed by Gaussian statistics and (2) the detection scheme is through homodyne beating.

$$P_i(\omega) = \frac{1}{2\pi} \int_{-\infty}^{\infty} e^{i\omega\tau} C_i(\tau) d\tau \quad (1)$$

where the current autocorrelation function is expressed as

$$C_i(\tau) = e \langle i \rangle \delta(\tau) + \langle i^2 \rangle g^{(2)}(\tau) \quad (2)$$

$$g^{(2)}(\tau) = 1 + |g^{(1)}(\tau)|^2 \quad (3)$$

$$g^{(1)}(\tau) = I_1 e^{-\Gamma_1|\tau|} + I_2 e^{-\Gamma_2|\tau|} \quad (4)$$

$$\Gamma_i = D_i q^2, \quad q = (4\pi/\lambda') \sin(\theta/2)$$

Here, the electronic charge is denoted by e , the mean photocurrent $\langle i \rangle$, Delta function $\delta(\tau)$, the mean square

photocurrent $\langle i^2 \rangle$, and the normalized intensity autocorrelation function $g^{(2)}(\tau)$ is given by the Siegert relation, [16] eq (3). The normalized field autocorrelation function $g^{(1)}(\tau)$ is expressed by a linear combination of two exponential decays with the time constants Γ_1 and Γ_2 , which are proportional to the respective diffusion coefficients, D_1 and D_2 , and the corresponding intensity factors I_1 and I_2 . The wavelength of the light in the scattering medium is denoted by λ' . Combining eqs. (1) through (4), we obtain the power spectrum in the broadened frequency scale from the incident angular frequency ω_0 , i.e., $\nu \equiv (\omega - \omega_0)/2\pi$;

$$P_i(\nu \geq 0) = e \langle i \rangle / \pi + \langle i^2 \rangle \delta'(\nu) + \frac{\langle i^2 \rangle}{\pi^2} I_1^2 \left\{ \frac{\Delta\nu_{1/2}^{(1)}}{\nu^2 + (\Delta\nu_{1/2}^{(1)})^2} + 2 \left(\frac{I_2}{I_1} \right) \frac{1/2 (\Delta\nu_{1/2}^{(1)} + \Delta\nu_{1/2}^{(2)})}{\nu^2 + [1/2 (\Delta\nu_{1/2}^{(1)} + \Delta\nu_{1/2}^{(2)})]^2} + \left(\frac{I_2}{I_1} \right)^2 \frac{\Delta\nu_{1/2}^{(2)}}{\nu^2 + (\Delta\nu_{1/2}^{(2)})^2} \right\} \quad (5)$$

$$\Delta\nu_{1/2}^{(i)} = \frac{D_i q^2}{\pi} \quad (6)$$

where $\delta'(\nu)$ is defined through

$$\int_{-\infty}^{\infty} \delta'(\nu) d\nu = 1$$

The first term in the RHS of eq. (5) represents the shot-noise level, the second term the dc contribution, and the third the double-Lorentzian spectral profile. Thus fitting to the double-Lorentzian profile of an observed power spectrum involves five parameters; they are (1) the shot-noise level, (2) the constant total intensity factor of the spectral portion $I_1^2 \langle i^2 \rangle / \pi^2$, (3) the halfwidth of the first component $\Delta\nu_{1/2}^{(1)}$, (4) the halfwidth of the second one $\Delta\nu_{1/2}^{(2)}$, and (5) the intensity ratio of the two components I_2/I_1 . We adopt the convention for designating the halfwidth of the slower moving component as $\Delta\nu_{1/2}^{(1)}$ and of the faster one as $\Delta\nu_{1/2}^{(2)}$ so that $\Delta\nu_{1/2}^{(2)} > \Delta\nu_{1/2}^{(1)}$.

The calibration of the double-Lorentzian analysis scheme was accomplished as follows. A binary mixture of polystyrene latex spheres was prepared by combining spheres having nominal diameters of 0.091 μm and 0.810 μm , in weight ratio of 98/2, i.e., 2 percent of the large spheres contaminating the principal component. The experimental power spectra acquired at different angles were analyzed according to eq (5) and $\Delta\nu_{1/2}^{(1)}$ and $\Delta\nu_{1/2}^{(2)}$ were determined. Four sets of the halfwidth values obtained at four different scattering angles provided two linear plots from which the diffusion coefficients

of the two spheres were determined according to eq (6), and found to be in complete agreement with those predicted by the Stokes law within 3 percent. A parallel experiment with 16 percent of the large sphere gave the analysis result which was indistinguishable from a solution consisting of pure 0.819 μm latex spheres; the single Lorentzian analysis was good enough. Thus we can extract the halfwidth of the smaller component of a binary mixture if the larger particles are present in about 2 percent or less when their diameter ratio is about 1/9.

3. Results and Discussion

The spectra at 45° of the 45S and 50S preparations are displayed in figures 1 and 2 respectively. In each figure, the upper part shows the experimental data overlaid on the fitted single-Lorentzian (chained curve) and the double-Lorentzian (solid curve) profiles, and the lower part indicates the corresponding normalized residues for the two types of profile. The residue plots clearly demonstrate the successful representation of the observed data by the double-Lorentzian scheme in each case. Similar analysis was effected for all observed spectra and the same conclusion was drawn for every spectrum. In tables I and II we collect the halfwidth data together with the intensity ratios (I_2/I_1) extracted from the double-Lorentzian analysis. Upon reducing all halfwidths to those in water at 20 °C, we determined the diffusion coefficients of the 45S and 50S states of the large ribosomal subunit and those of the contaminant particles via eq (6) at the hydrodynamic standard condition. In figures 3 and 4 we plot the reduced halfwidth of the principal components at different angles against q^2 for 45S and 50S preparations respectively. The error bar at each scattering angle represents the ranges of $\Delta\nu_{1/2}$ required for the 95 percent confidence limit of the fitted spectral profile. In addition, we also present in Fig. 4 the corresponding plot for the contaminating component of the 50S subparticles; the error bars are not shown for this case because they are comparable to the size of halfwidth data points (asterisk). From these plots we calculate the diffusion coefficients of all four components:

$$D_{20^\circ, w} (45S) = (1.79 \pm 0.12) \times 10^{-7} \text{ cm}^2/\text{sec.}$$

$$D_{20^\circ, w} (45S \text{ cont.}) = (2.22 \pm 0.30) \times 10^{-8} \text{ cm}^2/\text{sec.}$$

$$D_{20^\circ, w} (50S) = (1.91 \pm 0.06) \times 10^{-7} \text{ cm}^2/\text{sec.}$$

$$D_{20^\circ, w} (50S \text{ cont.}) = (2.99 \pm 0.14) \times 10^{-8} \text{ cm}^2/\text{sec.}$$

The uncertainty in each case is estimated by the 95 percent confidence interval for the mean value from the estimated

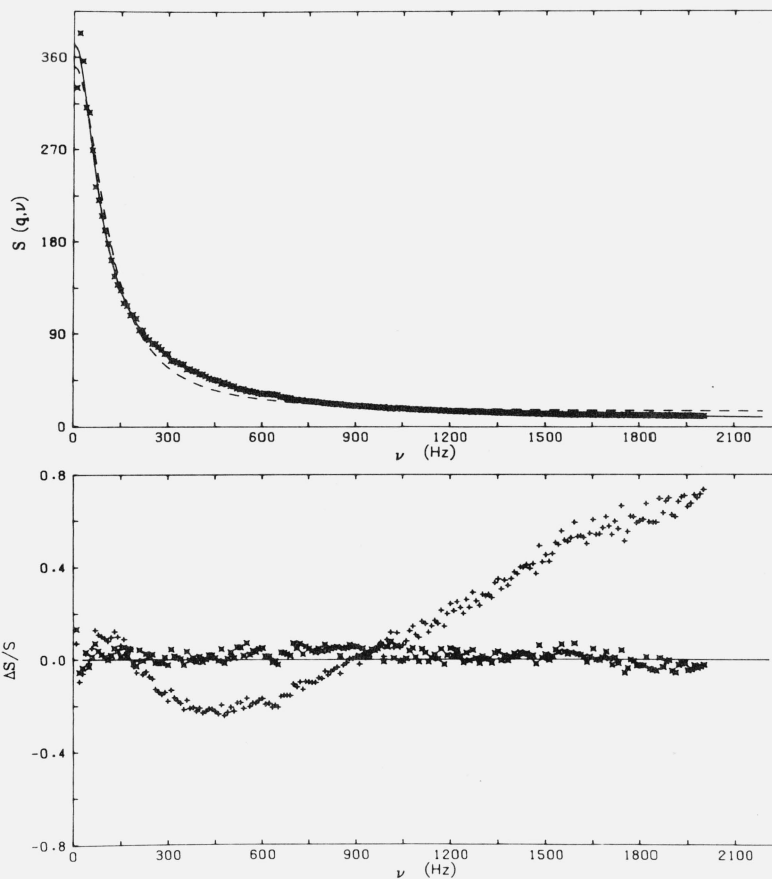


FIGURE 1. Upper: The observed power coefficients at 45° scattering angle of the 45S preparation vs the broadened frequency ν (Hz); solid and dashed curves represent the fitted double-Lorentzian and single-Lorentzian profiles respectively.

The ordinate is in arbitrary units.

Lower: The normalized residuals for the two analysis schemes vs ν (Hz); \times for the double-Lorentzian and $+$ for the single-Lorentzian scheme.

standard deviation and Student's t-value at $\alpha = 0.05$. The concentration dependence of the diffusion coefficient was not examined since its absence up to $0.6 \text{ mg}\cdot\text{ml}^{-1}$ for the subunit has been verified by Koppe [17] and it seems reasonable to assume that similar behavior would apply to the 45S state.

Setting aside for the moment the nature and sources of the contaminant particles, we proceed with the discussion of the ribosomal subunits. The mean value of $D_{20^\circ, w}$ for the 50S subunit is in good accord with those obtained by Tissieres *et al.* [18] and Serdyuk *et al.* [3] with use of the conventional techniques, as well as that by Koppel [17] who used the same technique as ours. On the other hand the uncertainty in our determination is greater than the one in Koppel's work by a factor of two; we estimate 3.2 percent whereas Koppel quotes 1.6 percent. The difference is attributable to the purity of his sample which, unlike ours, appeared to be free of contami-

nants; he observed single exponential decay of the photocurrent autocorrelation function which is equivalent to single Lorentzian profile in frequency domain. Thus our study seemingly attests the success of Koppel's ingenious scheme to effect the scattering with a pure sample at varying concentrations within a single cell. It is interesting to note that the two different signal processing routes, direct Fourier transformation in our case and photon count autocorrelation in Koppel's case, gave rise to an identical result although we could perform detailed statistical analysis with 200 data points for each spectrum while similar analysis might not have been possible with 20 data points (in a 24-channel correlator) by Koppel. In terms of the signal to noise ratio, the two procedures have been proven to be equivalent [19].

To the best of our knowledge, the diffusion coefficient of the 45S state of the large subunit has not been reported

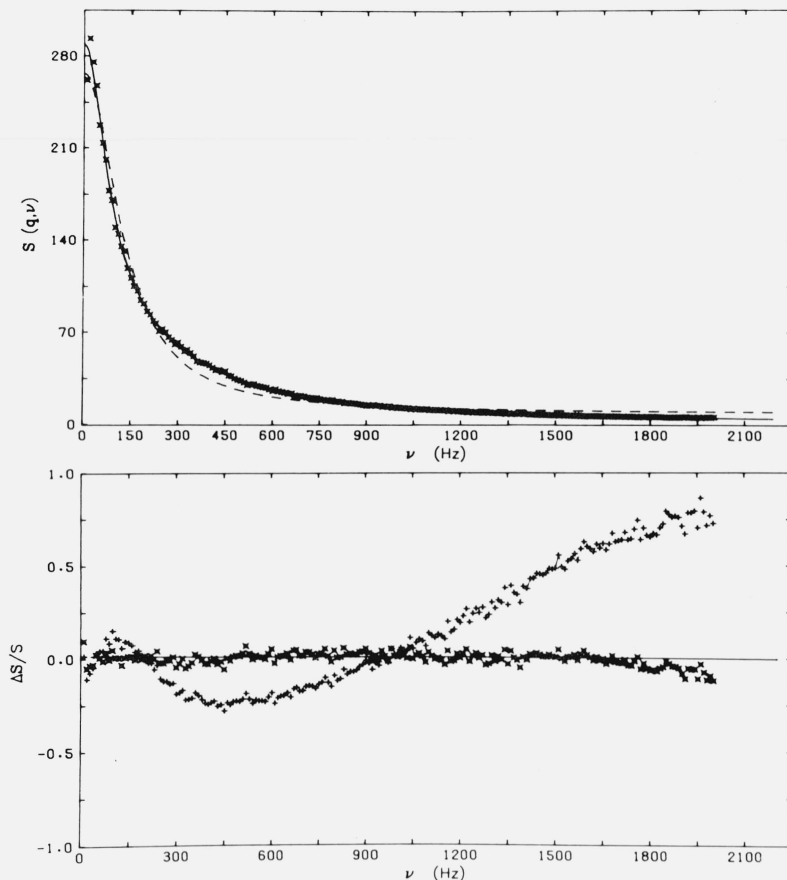


FIGURE 2. Upper: The observed power coefficients at 45° scattering angle of the 50S preparation vs the broadened frequency ν (Hz); solid and dashed curves represent the fitted double-Lorentzian and single-Lorentzian profiles respectively.

The ordinate is in arbitrary units.

Lower: The normalized residuals for the two analysis schemes vs ν (Hz); \times for the double-Lorentzian and $+$ for the single-Lorentzian scheme.

heretofore in the literature. The uncertainty in the final value however seems unusually large, amounting to nearly 8 percent. Sources of the large error bound are unclear; the intensity ratios in the 45S are quite comparable to those in the 50S subunit which would rule out the possibility of greater contamination in the 45S case. A question we now face is: Is the difference in the mean values of the two coefficients $[D(50S)-D(45S) = 0.12 \times 10^{-7} \text{ cm}^2/\text{sec}]$ statistically significant? To this end we evaluate a 95 percent confidence interval for the true underlying difference [20]. We find (0.013, 0.227), which does not include zero. Therefore, we may conclude that difference between the 50S and 45S means is positive, i.e., that the difference is statistically significant at the 5 percent level of significance. Accepting the difference to be significant, we might conclude that the molecular weights of two states are the same because

of the same ratio of sedimentation to diffusion coefficient provided that the partial specific volumes do not differ. Hill, Anderegg and van Holde [21] however found that the two states had different partial specific volumes but had the same molecular weight. Our results thus appear to contradict one of these two findings; either molecular weight is different or partial specific volume is identical. A closer analysis however yields consistency. Based on the error bounds of our diffusion coefficients and those of their partial specific volumes, we calculate according to the Svedberg equation the molecular weights of two states as $(1.73 \pm 0.16) \times 10^6 \text{ g/mol}$ ($s_{20,w} = 45.2 \times 10^{-13} \text{ sec}$) and $(1.55 \pm 0.07) \times 10^6 \text{ g/mol}$ ($s_{20,w} = 50.2 \times 10^{-13} \text{ sec}$) respectively for 45S and 50S subunits. Hence, the two molecular weights are the same within experimental error. We should note here that the molecular weights, by sedimentation equilibrium, reported

TABLE 1. The results of double-Lorentzian analyses for the 45S state of the large ribosomal subunit solution:

Angle (degree)	Temp (°C)	$\Delta\nu_{1/2}^{(1)}$ (Hz)	$\Delta\nu_{1/2}^{(2)}$ (Hz)	$\Delta\nu_{1/2}^{(2)}/\Delta\nu_{1/2}^{(1)}$	I_2/I_1	(a) $(P_2/P_1)_s$	(b) $(P_2/P_1)_{\text{calc}}$
45°	27.3 (20.0.w)	85.0 (72)	736 (621)	8.63	0.397	1.21	1.21
60°	27.3	159 (133)	1150 (971)	7.30	.568	1.73	1.39
75°	27.1	231 (195)	1754 (1487)	7.63	.745	2.27	1.64
90°	26.8	329 (281)	2452 (2093)	7.45	.882	2.69	1.96
110°	26.3	340 (293)	2843 (2453)	8.37	.980	2.99	2.51

After 0.1 μm Nuclearpore† filtration:

60°	— 25.8	165 (144)	1271 (1109)	7.70	1.400		
-----	--------	--------------	----------------	------	-------	--	--

(a) Scaled (I_2/I_1) to match $(P_2/P_1)_{\text{calc}}$ at 45°.

(b) Calculated from $P(q, R) = \left[\frac{3}{q^3 R^3} (\sin qR - qR \cos qR) \right]^2$ for a spherical particle with a radius R and the Stokes law, $R = \frac{kT}{6\pi\eta_0 D}$ where kT has the usual meaning, η_0 is the viscosity of solvent, and D the observed diffusion coefficient.

TABLE 2. The results of double-Lorentzian analyses for the 50S state of the large ribosomal subunit solution:

Angle (degree)	Temp (°C)	$\Delta\nu_{1/2}^{(1)}$ (Hz)	$\Delta\nu_{1/2}^{(2)}$ (Hz)	$\Delta\nu_{1/2}^{(2)}/\Delta\nu_{1/2}^{(1)}$	I_2/I_1	(a) $(P_2/P_1)_s$	(b) $(P_2/P_1)_{\text{calc}}$
30°	23.6 (20.0.w)	33.2 (30.5)	313 (287)	9.41	0.313	1.05	1.05
45°	23.8	86.5 (79.0)	679 (620)	7.85	.528	1.77	1.11
60°	24.3	184 (166)	1180 (1066)	6.41	.669	2.24	1.19
75°	24.7	278 (249)	1695 (1517)	6.10	.836	2.80	1.30
90°	25.3	403 (355)	2536 (2239)	6.30	.873	2.93	1.43
110°	25.7	504 (440)	3219 (2816)	6.39	.902	3.03	1.63

(a) Scaled (I_2/I_1) to match $(P_2/P_1)_{\text{calc}}$ at 30°.

(b) As in table I.

by Hill et al. are $(1.58 \pm 0.08) \times 10^6$ g/mol (45S) and $(1.55 \pm 0.05) \times 10^6$ g/mol (50S), whereby the absolute values of molecular weight by two experiments are also in agreement. From these considerations, it is quite plausible that the two states have the same mass but differ in their conformations such that a slight change in geometric eccentricity (or axial ratio) is reflected in their hydrodynamic parameters.

We now turn to the contaminants. As indicated above we really do not know where these come from. They might be the unfolded forms or large aggregates of the subunits though so small in amount that the Schlieren optics was not sensitive enough to detect them. The fact that the impurity component was representable by a Lorentzian profile (with $\Delta\nu_{1/2}^{(1)}$) cannot constitute the necessary condition for its monodispersity.

Any collection of components if present in small amount should have been fitted by a seemingly well defined one in the double-Lorentzian scheme, particularly when their diffusion coefficients are far different from that of the majority of scattering elements. Those solutions filtered through 0.1 μm Nuclearpore* filter gave rise to a larger intensity ratio I_2/I_1 , indicating that the contaminants could be removed, at least partially, upon filtration; they were not in equilibrium with the principal component. An example of this is provided in table I. While we cannot be sure of its character or sources without further study, it is possible to estimate its approximate mass ratio to the principal component. In addition, we can say something about its axial ratio compared to the subunit particles.

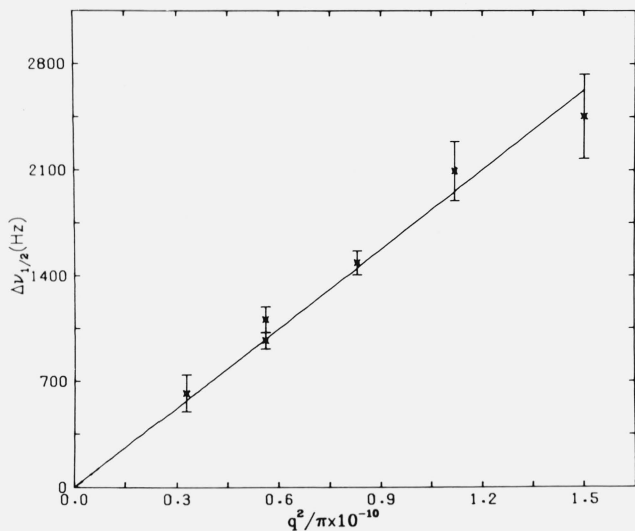


FIGURE 3. The reduced spectral halfwidth (20°C, water) for the principal component of the 45S preparation is plotted against q^2/π .

The error bars cover the 95% confidence interval about the mean halfwidth determined by the double-Lorentzian method at each scattering angle.

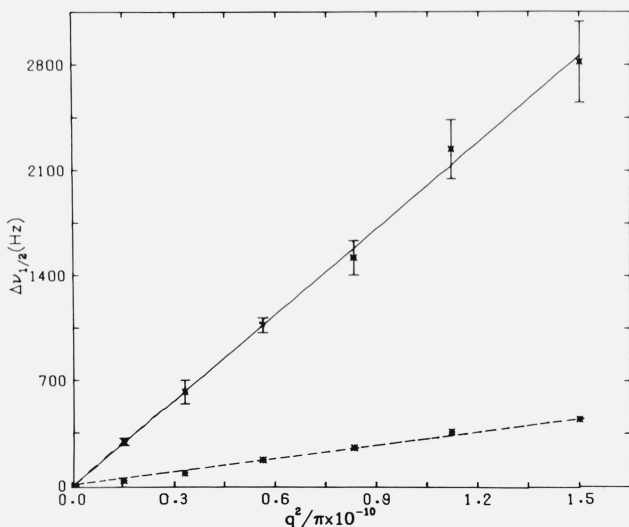


FIGURE 4. The reduced spectral halfwidth for the principal and contaminant components of the 50S preparation are plotted against q^2/π .

The error bars in the $\Delta\nu_{1/2}^2$ plot cover the 95% confidence interval about the mean halfwidth determined by the double-Lorentzian method at each scattering angle.

The mass ratio is estimated as follows. The intensity ratio is expressed by

$$\frac{I_2}{I_1} = \frac{K_2 M_2 c_2 P_2(q, R_2)}{K_1 M_1 c_1 P_1(q, R_1)} \quad (7)$$

where K_2 is proportional to the refractive index increment of the i th component (over the buffer), M_i is the molecular

weight, c_i the concentration in mass per unit volume, P_i the particle scattering function and R_i the linear dimension of the same component. In order to estimate the mass ratio c_1/c_2 , we need to make the following assumptions. They are: (1) $K_2 = K_1$, (2) $P_i(q, R_i) \approx 1$ at $30^\circ \sim 45^\circ$ scattering angle region, which might be low enough to allow such an assumption, and (3) M_2 is proportional to D_i^{-3} , which is equivalent to adopting the solid sphere model. From the last assumption, M_2/M_1 are estimated as 1.9×10^{-3} and 3.8×10^{-2} for the 45S and 50S states, respectively. The mass ratios c_1/c_2 are then computed from eq (7) as 5.8×10^{-3} ($\sim 0.6\%$) and 1.3×10^{-2} ($\sim 1.5\%$) for the 45S and 50S preparations, respectively, indicating only a small fraction of the large contaminants in each preparation. A similar situation was encountered by Chen *et al.* [23] in a recent study of dipalmitoyl phosphatidylcholine vesicles.

The relative shapes of the principal and contaminant components may be deduced as follows. Since the only scattering angle dependent term in eq (7) is $P_i(q, R_i)$, the observed I_2/I_1 ratio should be directly proportional to P_2/P_1 . Meantime, one can calculate the ratios P_2/P_1 assuming the sphere model for both components. We then compare them to the intensity ratio I_2/I_1 ; we scale I_2/I_1 so as to match the calculated P_2/P_1 at the lowest angle and examine the angular dependences of the scaled ratio, $(P_2/P_1)_s$ vis-a-vis the calculated one, $(P_2/P_1)_{\text{calc}}$. These are collected in the tables. It is apparent that $(P_2/P_1)_s$ increases with the scattering angle faster than $(P_2/P_1)_{\text{calc}}$, particularly with the 50S preparation. Thus we conclude that the principal ribosomal subunit component is more asymmetric than the contaminant component because the particle scattering factor $P(q, R_i)$ for a sphere decays most rapidly with q among the uniform density particles [24] and any asymmetry in the particle shape necessarily reduces the angular dependence of $P(q, R_2)$. Our conclusion however must be moderated if the two components were to differ in the uniformity of particle density.

This work is in part supported by the Graduate School of the University of Wisconsin. One of us (I.N.S.) wishes to acknowledge the hospitality tendered to him by U.S. National Academy of Sciences under USA-USSR Intergovernment Agreement on Scientific Exchange.

4. References

- [1] Pecora, R. (1972) *Ann. Rev. Biophys. Bioeng.* **1**, 257-276; Berne, B. J. and Pecora, R. (1976) *Dynamic Light Scattering* (Wiley, New York).
- [2] Carlson, F. D. (1975) *Ann. Rev. Biophys. Bioeng.* **4**, 243-264.
- [3] Tanford, C. (1961) *Physical Chemistry of Macromolecules* (John Wiley, New York) Chapter 6.
- [4] Serdyuk, I. N., Smirnov, N. I., Ptitsyn, O. B. and Fedorov, B. A. (1970) *FEBS Lett.* **9**, 324-326.
- [5] Barger, C. B. (1973) *Appl. Phys. Lett.* **23**, 379-381.

- [6] Lee, S. P. and Chu, B. (1974) *ibid.* **24**, 261-263.
- [7] Barger, C. B. (1974) *J. Chem. Phys.* **61**, 2134-2138.
- [8] Chen, F. C., Tscharnuter, W., Schmidt, D., and Chu, B. (1974) *ibid.* **60**, 1675-1676.
- [9] Brown, J. C., Pusey, P. N., and Dietz, R. (1975) *ibid.* **62**, 1136-1144.
- [10] Brehm, G. A. and Bloomfield, V. A. (1975) *Macromolecule* **8**, 663-665.
- [11] Koppel, D. E. (1972) *J. Chem. Phys.* **57**, 4814-4820.
- [12] Gavrilova, L. P., Ivanov, D. A., and Spirin, A. S. (1966) *J. Mol. Biol.* **16**, 473-489.
- [13] Shaya, S. A., Han, C. C.-C., and Yu, H. (1974) *Rev. Sci. Instrum.* **45**, 280-287.
- [14] Cummins, H. Z. and Swinney, H. L. (1970) *Progress in Optics*, ed. E. Wolf (North-Holland, Amsterdam) Vol. **VIII**, 133-200.
- [15] Ryshpan, J., NREG Subroutine, The University of Wisconsin MACC; Reference Manual, March 1972.
- [16] Jakeman, E. (1974) *Photon Correlation and Light Beating Spectroscopy*, ed. H. Z. Cummins and E. R. Pike (Plenum Press, New York) 75-149.
- [17] Koppel, D. E. (1974) *Biochemistry* **13**, 2712-2719.
- [18] Tissieres, A., Watson, J. D., Schlessinger, D., and Hollingworth, B. R. (1959) *J. Mol. Biol.* **1**, 221-233.
- [19] Degiorgio, V. and Lastovka, J. (1971) *Phys. Rev. A* **4**, 2033-2050.
- [20] The sum of squared deviations from the first (50S) and second (45S) sample means are 0.0163 and 0.0384 10^{-14} cm^4/sec^2 respectively, with 5 ($n_1 = 6$ angles) and 4 ($n_2 = 5$ angles) degrees of freedom respectively. Thus the pooled estimate of the (assumed) common standard deviation is $S = [(0.0163 + 0.0384)/9]^{1/2} = 0.0781 \cdot 10^{-7}$ cm^2/sec , with 9 degrees of freedom. Consequently 95% confidence limits for the true mean difference are given by,
- $$(D_1 - D_2) \pm 2.262S \sqrt{\frac{1}{n_1} + \frac{1}{n_2}},$$
- where 2.262 is the two-tail 5 percent significance level of Student's *t* for 9 degrees of freedom, that is, by
- $$0.12 \pm 2.262 \times 0.0781 \sqrt{\frac{1}{6} + \frac{1}{5}} = 0.12 \pm 0.107 \cdot 10^{-7} \text{cm}^2/\text{sec}$$
- (See, for example M. G. Natrella, *Experimental Statistics*, NBS Handbook 91, section 3-3.1-1.)
- [21] Hill, W. E., Andoregg, J. W., and van Holde, K. E. (1970) *J. Mol. Biol.* **53**, 107-121.
- [22] Svedberg, T. and Pedersen, K. O. (1940) *The Ultracentrifuge* (Oxford University Press, New York).
- [23] Chen, F. C., Chrzesczyk, A., and Chu, B. (1976) *J. Chem. Phys.* **64**, 3403-3409.
- [24] Kerker, M. (1969) *The Scattering of Light and Other Electromagnetic Radiation* (Academic, New York) pp. 482-485.